ADRC-LSE Control of a Dual-Star Induction Motor Powered by a Dual 3-level NPC Inverter

Darsouni Zakaria[(1)*], Rezgui Salah Eddine,Rebahi Fares,Hocine Benalla, Khalil Nebti
[(1)] Laboratory of Electrotechnics of Constantine(LEC), Frères Mentouri Constantine 1 University, Algeria
*Darsounizaki@gmail.com

Abstract: In the context of electric vehicle propulsion drives, this paper presents anActive disturbances Rejection Control (ADRC) strategyapplied to a Dual Star Induction Motor (DSIM)powered by dual 3 levels inverter type NPC. The proposed method focuses on enhancing the Active Disturbance Rejection Control (ADRC) method by integrating Least Squares Estimation, establishing a direct relationship between the control law and the necessary frequency for the DSIM to turn in the exact speed whatever the load torque applied. The ADRC with Least Squares Estimation is compared with Field-Oriented Control (FOC) to evaluate their performance in tracking reference speed and stabilizing time. Additionally, another test is conducted to assess the ADRC's ability to reject disturbances. Results from the simulation demonstrate the effectiveness of ADRC with Least Squares Estimation, showcasing its potential for optimizing DSIM control in electric vehicle applications, thereby contributing to enhanced efficiency and stability.

Keywords: DSIM (Dual Star Induction Motor); FOC (Field Oriented Control); ADRC (Active disturbances Rejection Control); NPC (Neutral Point Clamped); LSE (Least Squares Estimation); EV (Electrical Vehicle).

1. INTRODUCTION

In the realm of electric vehicle propulsion systems, there exists a diverse selection of motor topologies. These ones encompass DC motors, Asynchronous motors Brushless DC motors, Permanent magnet motors, Induction motors, and Switched reluctance motors [1,2]. To meet the demands of an efficient electric vehicle propulsion system, as outlined in references [3,4], several essential criteria must be met:

- The system must deliver high torque at low speeds for smooth starting and offer high power at higher speeds.
- It should include a broad speed range, including regions of constant torque and constant power.
- The system must maintain high efficiency across a wide range of speeds and torque levels.
- It should demonstrate high reliability and robustness under various vehicle operating conditions.
- Finally, it must be cost-effective to ensure its practicality and affordability in the market.

Numerous research studies have been conducted in this sector, exploring various motor types for electric vehicle (EV) propulsion. For instance, [5] utilized a DFIM in the traction chain, benefiting from its wide speed range. In a different approach, [6] employed a DC motor, a technology that traces its roots back to 1881 [7], Renowned for its high level of usability and extended operational lifespan. [2,8].

Another noteworthy motor type, the Synchronous Reluctance Permanent Magnet Machine, was the focus of [9]'s investigation. This machine combines elements of a synchronous reluctance machine (SynRM) with a permanent magnet synchronous machine (PMSM), offering superior performance compared to traditional induction motors and synchronous reluctance motors (IM and SRM). SRPM machines, exemplified by the Tesla Model 3, exhibit lower losses, high efficiency, and a high-power factor.

Similarly, [10] conducted research on asynchronous motors, a commonly adopted motor type in EVs. These motors are favored for their uncomplicated design and robust construction [11,12,13], resulting in reliable and highly efficient operation [11,14], even achieving up to 90% efficiency in adverse conditions [15]. Moreover, their simple control systems enable seamless startups, all while maintaining cost-effectiveness with low

production and maintenance expenses [11,13,14].

Industry attention is now delving into the intricacies of the multi-phase motor with specific attention to the Dual Star Asynchronous Motor (DSIM), a robust candidate primed to propel advancements in EV applications. It's characterized by two windings shifted by 30 electrical degrees, powered by a 6-phase inverter or 2 3-phase inverters. DSIMs are chosen for several compelling reasons. They exhibit significantly higher torque density compared to traditional induction motors, have the capacity to reduce harmonic content, and display exceptional reliability, even in the presence of phase faults [16,17,18]. Additionally, they offer power segmentation, effectively minimizing torque ripple, rotor losses, and mitigating harmonic current issues [19,20,21]. Renowned for their robustness and low maintenance requirements [20,21,22], DSIMs emerge as a prime candidate for the gradual replacement of induction motors, even in high-power industrial applications [16,23,24]. Another research made by [25] on five phase induction motor. These types of motors provide a high torque density, low torque ripple and flexible control, which make them another suitable case for propelling EVs.
To control such types of motors, there are numerous control techniques, including:

1.1. Field oriented Control (direct and indirect)

FOC

This technique is based on simplifying assumptions and mathematical transforms to make the asynchronous and synchronous motors similar to the direct current machine [26,27].these two methods allow control over the flow and torque of the machine, they have a better effect on the suppression of high order harmonics, setpoint monitoring with a respectable response time with great precision in the permanent regime [37,28,29], However it is fragile with respect to parametric variations [28,30], in addition the transformation of the quantities is based on an estimator which makes it very expensive. [31].

1.2. ACTIVE DISTURBANCES REJECTION CONTROL

ADRC

Active Disturbance Rejection Control is one of the most common nonlinear methods [32] for mitigating the effects of disturbances [33] and addressing control challenges in real-world applications [34].
The primary operating principle of the ADRC technique involves real-time compensation of the closed-loop system input with the estimated disturbance value. This transformation simplifies a relatively complex control system into a more straightforward one while allowing the closed-loop control system to achieve high performance [35,36].
Numerous studies have investigated this approach [35,37], yielding results that highlight several advantages. These advantages encompass beyond those mentioned above, effective disturbance rejection, precise reference tracking, swift stabilization times, independence from the requirement for a precise system model, real-time monitoring of both internal and external disturbances, as well as parameter uncertainties, thereby contributing to a high level of robustness.

This research focuses on the application of the DSIM within the context of electric vehicles. Specifically, the power of a dual inverter setup, recognized as the Neutral-Point-Clamped (NPC) configuration, is harnessed. For the purpose of ensuring precise control and maximizing the performance of the electric vehicle, an ADRC algorithm is implemented to command both inverters. Additionally, the integration of the least squares method (LSE) is carried out to

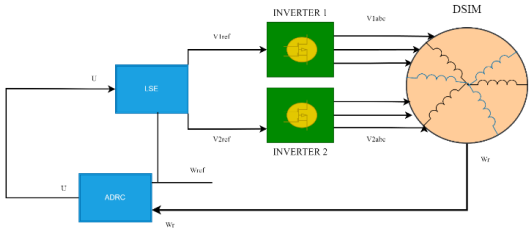

Fig.1. Block diagram of LSE-ADRC system for DSIM motor.

accurately determine the required frequencies for optimal operation of these inverters within the electric vehicle system as shown in Fig. 1.

2. MODELING OF THE DUAL STAR INDUCTION MOTOR (DSIM)

The spatial representation of windings of the dual star induction motor (DSIM) is illustrated on the Fig.2

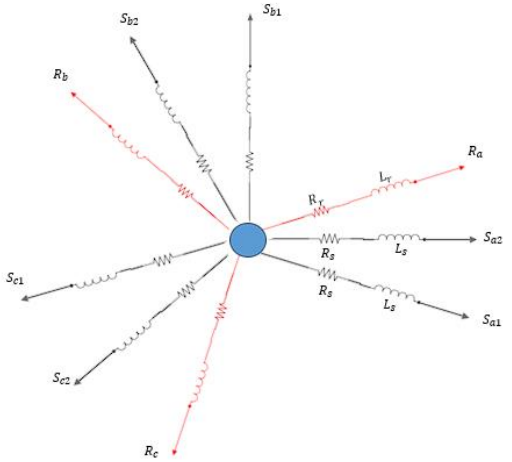

Fig.2. Schematic representation of the dual star induction motor

The dynamic of the DSIM in the reference dq can be divided into three categories [38]:

2.1. Electrical equations

$$\begin{cases} V_{ds1} = R_{s1}i_{ds1} + \frac{d}{dt}\emptyset_{ds1} - \omega_s\emptyset_{qs1} \\ V_{ds2} = R_{s2}i_{ds2} + \frac{d}{dt}\emptyset_{ds2} - \omega_s\emptyset_{qs2} \\ V_{qs1} = R_{s1}i_{qs1} + \frac{d}{dt}\emptyset_{qs1} + \omega_s\emptyset_{ds1} \\ V_{qs2} = R_{s2}i_{qs2} + \frac{d}{dt}\emptyset_{qs2} + \omega_s\emptyset_{ds2} \\ 0 = R_r i_{dr} + \frac{d}{dt}\emptyset_{dr} - (\omega_s - \omega_r)\emptyset_{qr} \\ 0 = R_r i_{qr} + \frac{d}{dt}\emptyset_{qr} + (\omega_s - \omega_r)\emptyset_{dr} \end{cases} \quad (1)$$

2.2. Magnetic equations

$$\begin{cases} \emptyset_{ds1} = L_{s1}i_{ds1} + L_m(i_{ds1} + i_{ds2} + i_{dr}) \\ \emptyset_{ds2} = L_{s2}i_{ds2} + L_{m(}i_{ds1} + i_{ds2} + i_{dr}) \\ \emptyset_{qs1} = L_{s1}i_{qs1} + L_{m(}i_{qs1} + i_{qs2} + i_{qr}) \\ \emptyset_{qs2} = L_{s2}i_{qs2} + L_{m(}i_{qs1} + i_{qs2} + i_{qr}) \\ \emptyset_{dr} = L_r i_{dr} + L_{m(}i_{ds1} + i_{ds2} + i_{dr}) \\ \emptyset_{qr} = L_r i_{qr} + L_{m(}i_{qs1} + i_{qs2} + i_{qr}) \end{cases} \quad (2)$$

2.3. Mechanical equations

The electromagnetic torque can be expressed by the following form:

$$C_{em} = p(\emptyset_{ds1}i_{qs1} - \emptyset_{qs1}i_{ds1} + \emptyset_{ds2}i_{qs2} - \emptyset_{qs2}i_{ds2}) \quad (3)$$

The rotation dynamic is given as follows:

$$\frac{d\Omega}{dt} = \frac{1}{j}(C_{em} - C_r - F_r) \quad (4)$$

3. Field Oriented Control (FOC)

Parameter	Value	Parameter	Value
R_s	3.72	L_r	0.006
R_r	2.12	L_m	0.4092
L_s	0.022	j	0.0625
P	1	F	0.001

Table 1. parameters of the DSIM

In order to decouple the control of the electromagnetic torque of the DSIM from the rotor flux, we align the rotor flux along the direct axis of Park's reference:

$$\begin{cases} \emptyset_{dr} = \emptyset_r \\ \emptyset_{qr} = 0 \end{cases} \quad (5)$$

The electrical equations will be:

$$\begin{cases} V_{ds1} = R_{s1}i_{ds1} + \frac{d}{dt}\emptyset_{ds1} - \omega_s\emptyset_{qs1} \\ V_{ds2} = R_{s2}i_{ds2} + \frac{d}{dt}\emptyset_{ds2} - \omega_s\emptyset_{qs2} \\ V_{qs1} = R_{s1}i_{qs1} + \frac{d}{dt}\emptyset_{qs1} + \omega_s\emptyset_{ds1} \\ V_{qs2} = R_{s2}i_{qs2} + \frac{d}{dt}\emptyset_{qs2} + \omega_s\emptyset_{ds2} \\ 0 = R_r i_{dr} + \frac{d}{dt}\emptyset_r \\ 0 = R_r i_{qr} + (\omega_s - \omega_r)\emptyset_r \end{cases} \quad (6)$$

The flux equations will be:

$$\begin{cases} \emptyset_{ds1} = L_{s1}i_{ds1} + L_m(i_{ds1} + i_{ds2} + i_{dr}) \\ \emptyset_{ds2} = L_{s2}i_{ds2} + L_{m(}i_{ds1} + i_{ds2} + i_{dr}) \\ \emptyset_{qs1} = L_{s1}i_{qs1} + L_{m(}i_{qs1} + i_{qs2} + i_{qr}) \\ \emptyset_{qs2} = L_{s2}i_{qs2} + L_{m(}i_{qs1} + i_{qs2} + i_{qr}) \\ \emptyset_r = L_r i_{dr} + L_{m(}i_{ds1} + i_{ds2} + i_{dr}) \\ \emptyset_{qr} = L_r i_{qr} + L_{m(}i_{qs1} + i_{qs2} + i_{qr}) = 0 \end{cases} \quad (7)$$

The electromagnetic torque:

$$C_{em} = p\frac{L_m}{L_m + L_r}(\emptyset_r(i_{qs1} + i_{qs2})) \quad (8)$$

4. ACTIVE DISTURBANCES REJECTION CONTROL

ADRC

Typically, the ADRC comprises three components: tracking differentiator (TD), extended state observer (ESO), and nonlinear state error feedback control law (NLSEF). Fig.3 illustrates the system schematic diagram of the classical ADRC.

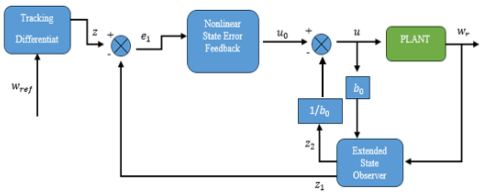

Fig.3. Diagram of Active disturbances rejection control

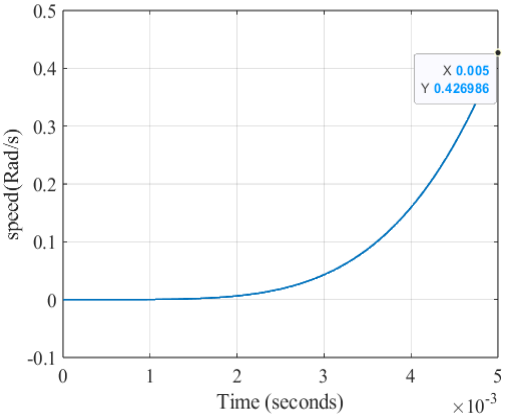

Fig.4. Speed response of DSIM with a 0.5 input in an open-loop configuration

For a more accurate representation of system dynamics, better disturbance estimation, and
the design of a control strategy that optimizes performance, stability, and robustness, selecting the appropriate model order is necessary, and for that the plant model is simulated in the open-loop configuration. Saturation limits of the duty cycle, ranging from 0 to 1, are assumed, and a step input.
The result is shown in figure 4. As can be seen, a typical shape for a second-order dynamic system is exhibited in the speed response.
The controlled object in the system will be set to:

$$\ddot{y} = f(t) + b_0\, u \quad (9)$$

$$a = \frac{2\Delta y}{\Delta t^2} = \frac{2(y(end) - y(0)}{(t(end) - t(0))^2}$$

$$= \frac{2 \times 0.426986}{(0.005 \times 10^{-3})^2} = 3.415888 \times 10^{10}$$

$$b_0 = \frac{a}{u} = 2 \times a$$

The state space model is as follow:

$$\begin{cases} \dot{x} = Ax + Bu + \begin{bmatrix} 0 \\ 0 \\ \dot{f}(t) \end{bmatrix} \\ y = Cx \end{cases} \quad (10)$$

While $A = \begin{bmatrix} 0 & 1 & 0 \\ 0 & 0 & 1 \\ 0 & 0 & 0 \end{bmatrix}$, $B = \begin{bmatrix} 0 \\ b_0 \\ 0 \end{bmatrix}$, $C = [1 \quad 0 \quad 0]$;

The ESO model can be expressed as follow:

$$\begin{cases} e = z_1 - w_r \\ z_1(k+1) = z_1(k) + T(z_2(k) + b_0 u + Ce_1) \\ z_2(k+1) = z_2(k) + Tz_2(k) \end{cases} \quad (11)$$

z_1 is the observed value of w_r , z_2 is the disturbance observed quantity of w_r and e_1 is the error between the observed value and the real value, u is the output value of ESO. While T is the discrete time constant, b_0 is the critical gain and C is constants.
The command law generated is:

$$\begin{cases} u_0 = (w_{ref} - z_1){w_c}^2 - 2w_c z_2 \\ u(t) = {(u_0 - z_3)}/{b_0} \end{cases} \quad (12)$$

While $z_3 = \hat{f}(t)$
The non-linear state error feedback is A modified PD controller (without the derivative part for the reference value r(t)), so the equation of u_0 will be:

$$u_0 = (w_{ref} - z_1)K_p - K_D z_2 \quad (13)$$

$K_p = {w_c}^2$; $K_D = 2w_c$.

5. APPLICATION ON THE DSIM

The generated ADRC law is subjected to a vector modelling process. This modelling process transforms the ADRC law into six distinct voltage references. These voltage references correspond to specific control parameters and serve as the inputs for our two 3-level Neutral-Point-Clamped (NPC) inverters as shows in fig. 5.

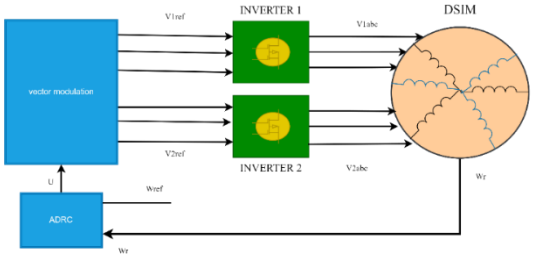

Fig.5.Application of ADRC on DSIM powered by two inverters

The following equations describe the vector modelling of the ADRC law:

$$\begin{cases} V_1 = u(t).\sin(2.\pi.f.t) \\ V_2 = u(t).\sin(2.\pi.f.t - \frac{2\pi}{3}) \\ V_3 = u(t).\sin(2.\pi.f.t + \frac{2\pi}{3}) \\ V_4 = u(t).\sin(2.\pi.f.t + \frac{\pi}{6}) \\ V_5 = u(t).\sin(2.\pi.f.t - \frac{\pi}{2}) \\ V_6 = u(t).\sin(2.\pi.f.t + \frac{5\pi}{6}) \end{cases}$$

$$\rightarrow normalization$$

$$\begin{aligned} V_{1n} &= V_1/(max|V_1|) \\ V_{2n} &= V_2/(max|V_2|) \\ V_{3n} &= V_3/(max|V_3|) \\ V_{4n} &= V_4/(max|V_4|) \\ V_{5n} &= V_5/(max|V_5|) \\ V_{6n} &= V_6/(max|V_6|) \end{aligned} \quad (14)$$

In the first phase of the application, a tracking test is conducted to evaluate the precision and stabilizing time of the ADRC. This test aims to assess how accurately the ADRC law tracks the desired trajectory and the time it takes to stabilize. In the second phase, a disturbance rejection test is performed by introducing resistive disturbances. This test is designed to evaluate the ADRC's ability to reject these disturbances, demonstrating its robustness and effectiveness in maintaining system stability and performance in the presence of external perturbations.

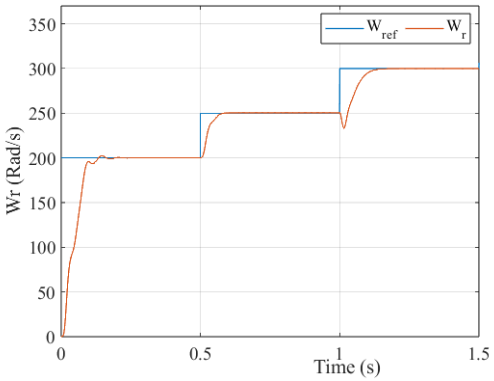

Fig.6. Speed Tracking of DSIM controlled by ADRC

In Figure 6, the Dual-Star Induction Motor demonstrates that employing the ADRC enables precise tracking of diverse speed references.

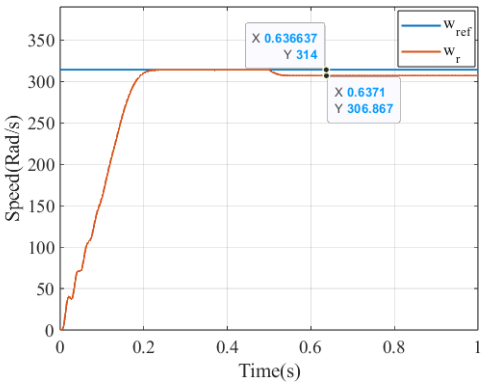

Fig.7. Speed of DSIM controlled by ADRC with 20N.m load

In Figure 7, the commencement of the Dual-Star Induction Motor (DSIM) and the subsequent application of a load equal 20N.m t=0.5 seconds are presented. The data clearly demonstrates that the ADRC implementation falls short in maintaining the targeted reference speed and effectively mitigating the introduced load disturbance.

The solution of this problem is presented in the next section when the least squares estimation method is introduced.

6. LEAST SQUARES ESTIMATION METHOD

LSE

The least squares method, initially introduced by Legendre in 1805 [39], stands as one of the most widely embraced estimation techniques, finding extensive application across a range of domains, including machine learning, system identification, and adaptive control, among others [40].

In this section, non-linear Least Squares Approach is used to derive a mathematical function that establishes a relationship among key parameters, including resistant torque, the control law generated by the Active Disturbance Rejection Control (ADRC) system, the reference frequency, and the requisite frequency for the two inverters. The primary objective is to achieve precise tracking of the reference speed while minimizing the impact of resisting torque in the shortest possible time.

The relationship between these variables identified as:

$$f(x) = a_4x^4 + a_3x^3 + a_2x^2 + a_1x + a_0 \quad (15)$$

While: $x = \frac{C_r}{U}$; $f(x) = f_r - f_m$

The operation commences by imposing a resistant torque vector upon DSIM, and at

each time step, we record both the generated control law and the measured frequency.

The conversion of speed to frequency is achieved through the utilization of the following formula: f(Hz)=(speed(rad/s))/2π.

The inverter frequency will be

$f_u = f_r + f(x)$ (16)

The least squares estimation method formula is:

$\mathrm{H} = (J^t * J)^{-1} * J^t * y$(17)

J: the Jacobian matrix

$J = \left[\frac{\partial f}{\partial a_4} \quad \frac{\partial f}{\partial a_3} \quad \frac{\partial f}{\partial a_2} \quad \frac{\partial f}{\partial a_1} \quad \frac{\partial f}{\partial a_0}\right]$ (18)

After the combination between equation (15) and (18):

$J = [x^4 \quad x^3 \quad x^2 \quad x \quad 1]$ (19)

After the calculation the results are as follows:

$$H = \begin{bmatrix} 7381502.1889 \\ 53567.2311 \\ 2048.2672 \\ 178.0575 \\ 0.014756 \end{bmatrix}$$

$a_4 = 7381502.1889$; $a_3 = 53567.2311$;
$a_2 = 2048.2672$; $a_1 = 178.0575$;
$a_0 = 0.014756$;

7. SIMULATION

In this section, a comprehensive simulation analysis is conducted usingMATLAB/Simulink as a chosen platform. MATLAB/Simulink offers a versatile and powerful environment for modelling and simulating complex control systems, making it an ideal tool for investigating the performance of our DSIM motor control system powered by two 3 levels NPC inverters.

In the first part of the simulation, the tracking accuracy and convergence time for various speed references will be evaluated between ADRC and FOC. In the second part, nominal resistive torque will be introduced for different speed values.

- Part 1:

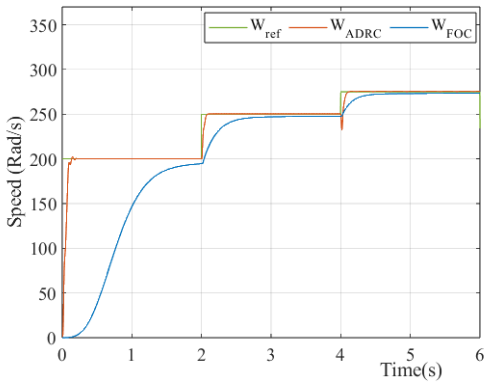

Fig.8. Measured Speed of DSIM at Different Reference Speed Values controlled by ADRC and FOC

The results in figure 8 can be divided into three phases as the table shows:

Table 2. comparison between ADRC and FOC in overshoot, precision and stabilizing time.

phase	Phase 1		Phase 2		Phase 3	
	ADRC	FOC	ADRC	FOC	ADRC	FOC
Over-shoot (%)	0	0	0	0	0	0
Precision (%)	100	98	100	98	100	98
Stabilizat-ion time (s)	0.2	2	0.2	1	0.2	1

- Part 2:

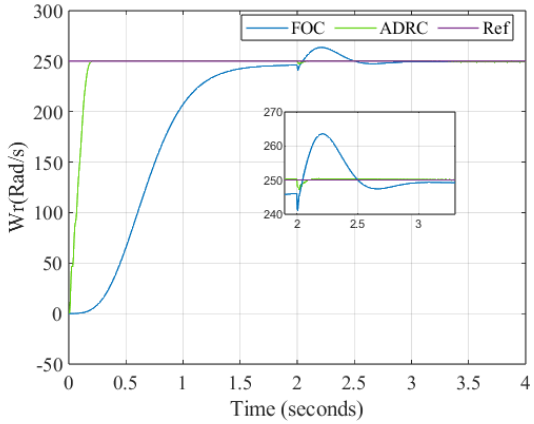

Fig.9. Comparison of DSIM Speed Control using ADRC and FOC with 20 N.m Applied Torque at a Speed Reference of 250 Rad/s

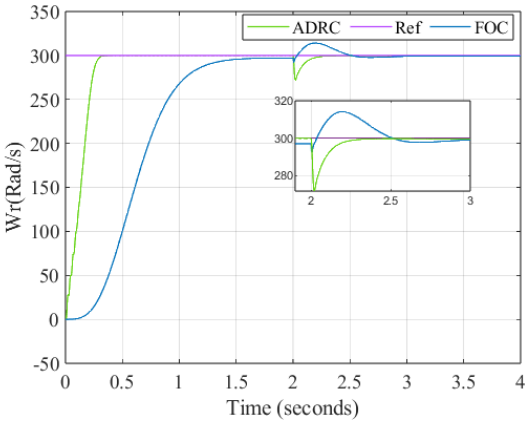

Figure 10. Comparison of DSIM Speed Control using ADRC and FOC with 20 N.m Applied Torque at a Speed Reference of 300 Rad/s

In the simulated control of a Dual star Induction Motor (DSIM) under varying speed references, the Active Disturbance Rejection Control (ADRC) and Field-Oriented Control (FOC) strategies were evaluated.

For a speed reference of 250 Rad/s, ADRC showcased remarkable performance by swiftly rejecting the load torque within 0.2 seconds and seamlessly returning to the reference speed with precise accuracy of 100%. On the other hand, FOC exhibited a longer response time, taking approximately 1 second to overcome the load torque and return to the reference speed with a high precision of 99%. As shown in fig. 9.

Advancing to a higher speed reference of 300 Rad/s, ADRC continued to impress with its efficiency, achieving load torque rejection in less than 0.5 secondsand maintaining a precise return to the reference speed with an accuracy of 100%. Conversely, FOC experienced a comparatively longer duration of around 1.5 seconds to reject the load torque and return to the reference speed with a slightly reduced precision of 99% as shown in fig. 10.

8. CONCLUSION

In industrial applications, as well as in the context of electric vehicles, our study demonstrates the remarkable effectiveness of the ADRC-LSE control method applied to the Dual Star Induction Motor (DSIM) powered by three-level NPC inverters. The DSIM exhibited impressive speed tracking capabilities, rapid convergence, and robust disturbance rejection. This combination of precision and reliability positions ADRC-LSE as a promising control solution, with the potential to enhance motor performance and efficiency across industries, while also contributing to the advancement of electric vehicle technology.

This approach holds significant potential for enhancing the efficiency and effectiveness of DSIM-powered electric vehicles, offering valuable insights into their practical applications and performance optimization in the realm of electric mobility.

9. NOMENCLATURE

P	number of pole pairs
j	the moment of inertia
R_{s1}, R_{s2}	stators resistance
L_{s1}, L_{s2}	stators inductances
$i_{ds1}, i_{qs1}, i_{ds2} i_{qs2}$	components of the stator currents in the dq axis
$V_{ds1}, V_{qs1}, V_{ds2}, V_{qs2}$	respectively stator voltages in the dq axis
L_r	rotor inductance
L_m	Mutual Inductance
$\emptyset_{ds1}, \emptyset_{qs1}, \emptyset_{ds2}, \emptyset_{qs2}$	Components of the stator flux in the dq axis
$\emptyset_{dr}, \emptyset_{qr}$	rotor flux in the dq axis
C_{em}	The Electromagnetic Torque
C_r	The Load Torque
F_r	The friction Coefficient
U	generated law by ADRC.
f_r	reference frequency.
f_m	measured frequency.
J	TheJacobian matrix

10. REFERENCES

[1]Hamza Ahmed, Sajjad Haider Zaidi PN, M. Farhan Khan. «A Comparative Study on Different Motors used in Electric Vehicles». Journal of Independent Studies and Research Computing. JISR-C, Volume 20, Issue 2, July-December 2022.

[2]Vasanthakumar S. «SELECTION OF MOTOR FOR AN ELECTRIC VEHICLE», Rajalakshmi Engineering College. 31 December 2021.

[3]Rahman, Z. 'An investigation of electric motor drive characteristics for EV and HEV propulsion systems'. SAE Technical Paper Series. Paper no. 2000-01-3062 (2000).

[4]Chan, C.C.: The state of the art of electric and hybrid vehicles. Proc. IEEE. 90(2), 247–275 (2002)

[5]Ahmed Chantoufi, Aziz Derouich, Najib El Ouanjli, Said Mahfoud1, Abderrahman El Idrissi, and Mohammed Taoussi. 'Direct Torque Control for Doubly Fed Induction Motor Driven Electric Vehicle'. Conference Paper · May 2023 DOI: 10.1007/978-3-031-29860-8_86.

[6]Toqeer Ahmed, Syed Tahir Mehboob, Muahmmad Qasim, Javeria Areej Khan, Sadiq Ahmad. 'Efficiency Improvement of Electric Vehicles by Using Winding-Less Rotor Based DC Motor'.

[7]Iqbal Husain. Electric and hybrid vehicles: design fundamentals. CRC Press, 2003.https://doi.org/10.3390/electronics12030539.

[8]Ammar Arif Ansari. “A Review of Different Motor Types and Selection of One Optimal Motor for Application in EV Industry”. Int. J. Elec. Power Eng., 16 (1): 1-7, 2022 E.

[9]Sousa, J.D.C.; Sousa, T.J.C.; Monteiro, V.; Afonso, J.L. ‘Traction System for Electric Vehicles Based on Synchronous Reluctance Permanent Magnet Machine’. Electronics 2023, 12, 539.

[10]Goolak, S.; Liubarskyi, B.; Riabov, I.; Lukoševi˘cius, V.; Keršys,A.; Kilikevi˘cius, S. Analysis of the Efficiency of Traction Drive Control Systems of Electric Locomotives with Asynchronous Traction Motors. Energies 2023, 16, 3689. https:// doi.org/10.3390/en16093689.

[11]Takahashi I., Noguchi. T.: “A new quick response and high efficiency strategy of an induction motor,” in Conf. Rec. IEEE-IAS Annu. Meeting, pp. 495–502, 1985.

[12]R. Pindoriya, B. Rajpurohit, R. Kumar and K. Srivastava, “Comparative analysis of permanent magnet motors and switched reluctance motors capabilities for electric and hybrid electric vehicles”, 2018 IEEMA Engineer Infinite Conference (eTechNxT), 2018.

[13]Di Tong, Zhen Guo, Yan-cheng Zhao, Shuang Chen, Ji-qiu Nai, Ming-hao Ye.” Efficiency Optimization of Asynchronous Motor with Particle Swarm Algorithm Incorporating Parameter Identification”. Journal of Physics: Conference Series 2522 (2023) 012003. IOP Publishing. doi:10.1088/1742-6596/2522/1/012003.

[14]Depenbrock. M.: “Direct self-control for high dynamics performance of inverter feed AC machines,” ETZ Arch.., vol. 7, no. 7, pp. 211–218, 1985.

[15]MatkarimIbragimov, DilmurodAkbarov, and IrodaTadjibekova.” Investigation of asynchronous electric motor winding in heating mode and drying mode to prevent moisture”. E3S Web of Conferences 365, 04019 (2023). https://doi.org/10.1051/e3sconf/202336504019.

[16]GhoulemallahBoukhalfa, SebtiBelkacem ,AbdesselemChikhi, Said Benaggoune.” Direct torque control of dual star induction motor using a fuzzy-PSO hybrid approach” Applied Computing and Informatics. https://doi.org/10.1016/j.aci.2018.09.001.

[17]K. Pien´ kowski.” Analysis and control of dual stator winding induction motor”. Arch. Electric. Eng. 61 (3) (2012) 421–438.

[18]Meliani Bouziane, Meroufel Abdelkader.” A Neural Network Based Speed Control of a Dual Star Induction Motor”. International Journal of Electrical and Computer Engineering (IJECE). Vol. 4, No. 6, December 2014, pp. 952~961.

[19]Layadi, N., Djerioui, A., Zeghlache, S., Houari, A., Benkhoris, M. F., Berrabah, F. "A Hybrid Fuzzy Sliding Mode Controller for a Double Star Induction Machine", In: 2018 International Conference on Communications and Electrical Engineering (ICCEE), El Oued, Algeria, 2018, pp. 1–6. https://doi.org/10.1109/CCEE.2018.8634439.

[20]Marouani, K., Baghli, L., Hadiouche, D., Kheloui, A., Rezzoug, A. "A New PWM Strategy Based on a 24-Sector Vector Space Decomposition for a Six-Phase VSI-Fed Dual Stator Induction Motor", IEEE Transactions on Industrial Electronics, 55(5), pp. 1910–1920, 2008. https://doi.org/10.1109/TIE.2008.918486.

[21]Sellah, M., Kouzou, A., Rezaoui, M. M. "Investigation of SVPWM Based Sliding Mode Control Application on Dual-Star Induction Motor and Dual Open-End Winding Induction Motor", PeriodicaPolytechnica Electrical Engineering and Computer Science, 66(1), pp. 80–98, 2022. https://doi.org/10.3311/PPee.17910.

[22]Khadar, S., Kouzou, A., Rezzaoui, M. M., Hafaifa, A. "Sensorless Control Technique of Open-End Winding Five Phase Induction Motor under Partial Stator Winding Short-Circuit", PeriodicaPolytechnica Electrical Engineering and Computer Science, 64(1), pp. 2–19, 2020. https://doi.org/10.3311/PPee.14306.

[23]Y. Zhao, T.A. Lipo “Space vector PWM control of dual three-phase induction machine using vector space decomposition”. IEEE Trans. Ind. Appl. 31 (5) (1995) 1100–1108.

[24]S. Basak, C. Chakraborty, ‘Dual stator winding induction machine, Problems, Progress, and Future’ Scope IEEE Trans. Ind. Electron. 62 (7) (2015) 4641–4652.

[25]Zeng, R.; Zhao, J.; Xiong, Y.; Luo, X. ‘Active Disturbance Rejection Control of Five-Phase Motor Based on Parameter Setting of Genetic Algorithm’. Processes 2023, 11, 1712. https://doi.org/10.3390/pr11061712.

[26]N. M. Babak "Commande vectorielle sans capteur mécanique des machines synchrones à aimants : Méthodes, convergence, robustesse, identification "en ligne" des paramètres", Thèse de doctorat, 2001.

[27]Zheng Guo, Jiasheng Zhang, ZhenchuanSun,Changming Zheng. ‘Indirect Field oriented control of three-phase Induction Motor Based On current source Inverter’. 13^th Global Congress On manufacturing and management p 588-594, GCMM 2016.

[28]Isa Eray A Kyol, Mehmet Turan Soylemez. ‘Postion sensorless field-oriented control of IPMSM under parameter uncertainties. IFAC 2017.

[29]R.Seliger, B. Köppen, P.M. Frank, M.A. El-sharkawi, ‘Self-tuning adaptative control for field-oriented controlled induction motors- a simulation study’ pp 505-510. IFAC 1991.

[30]G.W. Chang, J.P. Hepanha, A.S. Morse, M.S. Netto, R. Ortega. ‘Supervisory field-oriented control of induction motors with uncertain rotor resistance’.

[31]M. Pradeep Kumar, S. Sirisha and M. Chandramouly, ‘Design of Pmsm Base on DTC method with Mras’. International Journal of

Engineering Research and Applications, vol. 1, issue 3, Sep-Oct 2013, pp. 646-653.

[32]Jian Luo, Lichao Wang &Bingyou Liu (2021) "Low-speed control of PMSM based on ADRC + FOPID", Systems Science & Control Engineering, 9:1, 73-87, https://doi.org/10.1080/21642583.2020.1863279.

[34]GERNOT HERBST AND RAFAL MADONSKI." TUNING AND IMPLEMENTATION VARIANTS OF DISCRETE-TIME ADRC". Article in Control Theory and Technology. March 2023 DOI: 10.1007/s11768-023-00127-0.

[35]Li, Z.; Zhang, Z.;Wang, J.; Wang, S.; Chen, X.; Sun, H. 'ADRC Control System of PMLSM Based on Novel Non-Singular Terminal Sliding Mode Observer. Energies' 2022, 15, 3720. https://doi.org/10.3390/en15103720.

[36]Lin, P.;Wu, Z.; Liu, K.-Z.; Sun, X.-M. 'A Class of Linear–Nonlinear Switching Active Disturbance Rejection Speed and Current Controllers for PMSM'. IEEE Trans. Power Electron. 2021, 36, 14366 14382.

[37]Tan, L.; Liang, S.; Su, H.; Qin, Z.; Li, L.; Huo, J. Research on Amphibious Multi-Rotor UAV Out-of-Water Control Based on ADRC. Appl. Sci. 2023, 13, 4900. https://doi.org/10.3390/app13084900.

[38]Rachid ABDESSEMED. ' Modélisation et simulation des machines électriques ' édition paris (Ellipses), 2011.

[39]QingruiZhang. 'A Tutorial on Linear Least Square Estimation'. https://arxiv.org/abs/2211.15347v1. November 2022.

[40]Legendre, Adrien-Marie (1805). 'Nouvelles méthodes pour la détermination des orbites des comètes' [New Methods for the Determination of the Orbits of Comets] (in French), Paris : F. Didot, hdl:2027/nyp.33433069112559.